

Accepted Manuscript

In-vitro metabolomics to evaluate toxicity of particulate matter under environmentally realistic conditions

Francisco Sánchez-Soberón, Matthias Cuykx, Noemi Serra, Victoria Linares, Montserrat Bellés, Adrian Covaci, Marta Schuhmacher



PII: S0045-6535(18)31140-8

DOI: [10.1016/j.chemosphere.2018.06.065](https://doi.org/10.1016/j.chemosphere.2018.06.065)

Reference: CHEM 21597

To appear in: *ECSN*

Received Date: 19 March 2018

Revised Date: 7 June 2018

Accepted Date: 8 June 2018

Please cite this article as: Sánchez-Soberón, F., Cuykx, M., Serra, N., Linares, V., Bellés, M., Covaci, A., Schuhmacher, M., *In-vitro* metabolomics to evaluate toxicity of particulate matter under environmentally realistic conditions, *Chemosphere* (2018), doi: 10.1016/j.chemosphere.2018.06.065.

This is a PDF file of an unedited manuscript that has been accepted for publication. As a service to our customers we are providing this early version of the manuscript. The manuscript will undergo copyediting, typesetting, and review of the resulting proof before it is published in its final form. Please note that during the production process errors may be discovered which could affect the content, and all legal disclaimers that apply to the journal pertain.



1 ***In-vitro* metabolomics to evaluate toxicity of particulate matter under environ-**
2 **mentally realistic conditions**

3 Francisco Sánchez-Soberón¹, Matthias Cuykx², Noemi Serra³, Victoria Linares³, Montserrat Bellés³, Adrian
4 Covaci², Marta Schuhmacher^{1*}

5 ¹*Universitat Rovira i Virgili, Chemical Engineering Department, Environmental Analysis and Management*
6 *Group, Av. Països Catalans 26, 43007 Tarragona, Spain*

7 ²*Toxicological Center, Department of Pharmaceutical Sciences, University of Antwerp, Universiteitsplein 1,*
8 *2610 Antwerp, Belgium*

9 ³*Universtiat Rovira i Virgili, School of Medicine, Laboratory of Toxicology and Environmental Health, San*
10 *Lorenzo 21, 43201 Reus, Spain*

11 *Corresponding author: marta.schuhmacher@urv.cat

12 Declarations of interest: none

13 1

14

Abbreviations: ACN: Acetonitrile; CCOHS: Canadian Centre for Occupational Health and Safety; CERs: Ceramides; CHCl₃: Chloroform; Cho: Choline; CLs: Cardiolipins; Etn: Ethanolamine; EU: European Union; FA: Formic Acid; HAc: Acetic Acid; IC₅: 5% Inhibitory Concentration; IPA: Isopropanol; MeOH: Methanol; NH₄Ac : Ammonium Acetate; NH₄F: Ammonium Formate; LC-MS: Liquid Chromatography-Mass Spectrometry; P: Pulmonary; PBS: Phosphate Buffered Saline; PC: Polycarbonate; PCs: Phosphatidylcholines; PEMT: Phosphatidyl-Ethanolamine N-Methyltransferase; PEs: Phosphatidylethanolamines; PGs: Phosphatidylglycerols; PM: Particulate Matter; PSs: Phosphatidylserines; QC: Quality Control; Ser: Serine; TB: Tracheobronchial; TEHP: 2-ethylhexyl phosphate; TG: Triglycerides; US EPA: United States Environmental Protection Agency; WHO: World Health Organization.

15 Keywords

16 Particulate matter; Indoor sampling; A549; Cytotoxicity; HP-LC/MS; Metabolomics

17 Abstract

18 In this pilot study three fractions of particulate matter ($PM_{0.25}$, $PM_{2.5-0.25}$, and $PM_{10-2.5}$) were
19 collected in three environments (classroom, home, and outdoors) in a village located nearby an
20 industrial complex. Time-activity pattern of 20 students attending the classroom was obtained, and
21 the dose of particles reaching the children's lungs under actual environmental conditions (i.e. real
22 dose) was calculated via dosimetry model. The highest PM concentrations were reached in the
23 classroom. Simulations showed that heavy intensity outdoor activities played a major role in PM
24 deposition, especially in the upper part of the respiratory tract. The mass of $PM_{10-2.5}$ reaching the
25 alveoli was minor, while $PM_{2.5-0.25}$ and $PM_{0.25}$ apportion for most of the PM mass retained in the
26 lungs. Consequently, $PM_{2.5-0.25}$ and $PM_{0.25}$ were the only fractions used in two subsequent toxicity
27 assays onto alveolar cells (A549). First, a cytotoxicity dose-response assay was performed, and
28 doses corresponding to 5% mortality (LC_5) were estimated. Afterwards, two LC-MS metabolomic
29 assays were conducted: one applying LC_5 , and another applying real dose. A lower estimated LC_5
30 value was obtained for $PM_{0.25}$ than $PM_{2.5-0.25}$ (8.08 and 73.7 ng/mL respectively). The number of
31 altered features after LC_5 exposure was similar for both fractions (39 and 38 for $PM_{0.25}$ and $PM_{2.5-}$
32 0.25 respectively), while after real dose exposure these numbers differed (10 and 5 for $PM_{0.25}$ and
33 $PM_{2.5-0.25}$ respectively). The most metabolic changes were related to membrane and lung surfactant
34 lipids. This study highlights the capacity of PM to alter metabolic profile of lung cells at
35 conventional environmental levels.

36

37 1. Introduction

38 Particulate matter (PM) is recognized as one of the most harmful air pollutants (Megido et al.,
39 2016). PM consists of liquid droplets and solid fragments smaller than 10 μm suspended in the air,

40 whose size, chemical composition, and shape are varied (WHO, 2014). For regulatory purposes,
41 environmental agencies all over the world usually classify PM into two groups according to its size:
42 PM₁₀ (those particles having a diameter smaller than 10 µm, sometimes named as respirable) and
43 PM_{2.5} (smaller than 2.5 µm, also referred as fine) (European Commission and EU Parliament, 2008;
44 US EPA, 2016). Several studies agree that the smaller the PM, the more harmful it is, since it is
45 usually enriched in toxic components, such as polycyclic aromatic hydrocarbons (PAHs) and heavy
46 metals, and it can reach deeper parts of the respiratory system (Kelly and Fussell, 2016). In fact, it is
47 estimated that PM_{2.5} is responsible of more than 2 million premature deaths per year globally
48 (Donahue et al., 2016).

49 *In vitro* tests have been used to assess the toxicity of PM (Wu et al., 2018). The classical approach
50 in these assays consists of applying varying doses of toxicant on different cell types, and study
51 parameters such as cytotoxicity, genotoxicity, strength of cell junction or apoptosis (X. Cao et al.,
52 2015; Chen et al., 2017; Peixoto et al., 2017). Although it is possible to find examples of papers
53 focused on studying the effects of PM under realistic conditions (van Drooge et al., 2017), these
54 studies are conventionally used as a way of studying elicited effects of PM on cells for short term
55 exposures (usually 24 hours) and doses higher than those experienced in environmental conditions.

56 To have a better approach of observing changes in cells at low and real doses, omics sciences are a
57 powerful tool. Omics are a series of disciplines focused on studying the complete profile of genes
58 (genomics), mRNA (transcriptomics), proteins (proteomics), or metabolites (metabolomics) for a
59 given cell type or organism (Horgan and Kenny, 2011). Although nowadays papers applying
60 different omics methods on lung cells have been published, the number of studies assessing toxicity
61 of ambient PM by omics means is still low (Q. Huang et al., 2015; Líbalová et al., 2012; Longhin et
62 al., 2016; Vaccari et al., 2015; Wang et al., 2017; Wheelock et al., 2013; Zhang et al., 2017).
63 Furthermore, although some papers using omics techniques to evaluate PM toxicity under exposure
64 conditions typical of general population living in western countries can be found (Mesquita et al.,
65 2015), to the best of our knowledge there is no paper assessing such a thing onto pulmonary cells.

66 The aim of the present study is to have a deeper understanding of health effects on human lung cells
67 when exposed to PM under low dose and mid-term exposure conditions. To do so, three fractions of
68 PM ($PM_{10-2.5}$, $PM_{2.5-0.25}$, and $PM_{0.25}$) were collected in three different environments (outdoors, inside
69 a classroom, and inside a domestic living room) nearby an industrial area in the Tarragona County
70 (Catalonia, Spain). To calculate the exposure of kids attending the classroom, time-activity pattern
71 of children attending the school was gathered. Subsequently, a dosimetry model (MPPD) was used
72 to calculate real dose of PM reaching the children's lungs. To have an overview of the total toxicity
73 of the PM, a cytotoxicity assay was performed after exposing human alveolar cells (A549) to
74 different doses of those fractions of PM able to reach the lungs (i.e. $PM_{2.5-0.25}$ and $PM_{0.25}$). Finally,
75 to have a better insight of hazardous potential of these materials, a metabolomic assay was
76 performed by exposing the cells at LC_5 (concentration of PM causing a 5% mortality) and a real
77 dose of the two fractions during mid-term (72 h) exposure time.

78 2. Methods

79 2.1. Materials, chemicals, and standards

80 Polycarbonate (PC) filters for sampling were purchased from Whatman (Maidstone, UK). Lung
81 carcinoma cells A549 (ATCC[®] CCL-185TM), culture media and supplements,
82 methylthiazolyldiphenyl-tetrazolium bromide (MTT) reagent, and detergent reagent were obtained
83 from ATCC (Teddington, UK). Phosphate buffered saline (PBS), methanol (MeOH), and
84 acetonitrile (ACN) were obtained from Thermo Fisher (Waltham, MA, USA). Chloroform ($CHCl_3$),
85 isopropanol (IPA), ammonium acetate (NH_4Ac), acetic acid (HAc), formic acid (FA), and
86 ammonium formate (NH_4F) were obtained from Merck KGaA (Darmstadt, Germany). Chamber
87 slides, tributylamine (TBA), 2-ethylhexyl phosphate, and succinic acid-d4 were obtained from
88 Sigma-Aldrich (St. Louis, MO, USA). Cholesterol-d4, lauric acid-d3, and tryptophane-d5 were
89 obtained from CDN Isotopes (Pointe-Claire, Quebec, Canada).

90 2.2. PM sampling and extraction

91 Samples of PM_{10-2.5}, PM_{2.5-0.25} and PM_{0.25} were collected simultaneously from 2nd to 6th of May 2016
92 in Perafort (Tarragona province, Spain). This location is settled in a suburban area, where the air is
93 influenced by the presence of an industrial estate located 3 km south-west (Figure S1). This
94 industrial area comprises an oil refinery and several chemical companies (MAPAMA, 2018).
95 Samples were collected in three different environments: inside a classroom, inside a living room,
96 and outdoors. These environments were in the same village, within a 200 meters radius. The volume
97 of the classroom was 173.25 m³, and 20 students were attending the class during sampling. The
98 house living room had 40.43 m³ and was occupied by three nonsmoking people. Regarding the
99 outdoor sample, it was collected in the first-floor terrace of the same school at which the classroom
100 belongs. No ventilation was registered during the sampling period in the indoor environments.
101 Samples were collected onto (PC) filters using cascade impactors (SiotuasTM, SKC Inc. Eighty-
102 Four, PA, USA) connected to a pump (Leland Legacy, SKC). Two samplers were placed in every
103 environment, working simultaneously at a flow rate of 9 L/min. After 48 h, PC filters were replaced,
104 till having a total of 4 samples per fraction and environment. Before and after sampling, filters were
105 weighted several times till reaching a constant weight on a 10- μ g accuracy microbalance. Masses of
106 PM were calculated as the differences in filters weight before and after sampling. Particulate matter
107 concentrations in air were then calculated by dividing the masses by the total sampled air volume.
108 To extract PM from PC filters, these were submerged into tubes containing deionized water, shaken
109 for 20 min and sonicated for 10 min. Subsequently, filters were removed from the tubes, dried at
110 room temperature, and weighted again. The supernatants were centrifuged at 3500 rpm., freeze-
111 dried, and stored at -20 °C until further analysis. Extraction recoveries for PM ranged between 92
112 and 102%. Clean PC filters subjected to the same extraction procedure were used as negative
113 control.

2.3. Children activity pattern

114 To calculate the real dose of PM inhaled by children, physical activities performed in every
115 microenvironment as well as the duration of these activities were registered. 20 nine- to ten-year old
116 students attending the sampling room were asked to describe their daily routine. Their routine was
117 classified into 6 different activities: heavy exercise outdoors, light exercise outdoors, light exercise
118 at home, sitting at school, sitting at home, and sleeping time.

119 *2.4. Calculation of real doses*

120 Using the average measured PM levels and kids activity pattern as inputs, the deposition of the
121 three PM fractions was calculated for three regions of the respiratory tract (Head, Tracheobronchial
122 (TB), and Pulmonary (P)) by the use of a dosimetry model (MPPD v 2.11 (ARA, 2014)). To
123 calculate the real dose to use in the experiments, the total amount of PM reaching the pulmonary
124 region was divided by 32 m² to obtain the mass of PM per alveolar area for an 8 years old kid
125 (Dunnill, 1962). Then, this number was multiplied by the total surface of the chamber slide used for
126 growing the cells (4.2 cm²). All other parameters needed for the simulation were remained as
127 described previously (Sánchez-Soberón et al., 2015).

128 *2.5. Cell line and cytotoxicity assay*

129 Lung carcinoma cells A549 (ATCC[®] CCL-185[™]) have been extensively used in toxicity of lung
130 cells (L. Cao et al., 2015; Xu et al., 2013). To study the cytotoxicity of PM_{2.5-0.25} and PM_{0.25}, an
131 MTT assay was performed for each PM fraction separately (Roig et al., 2013). Cells were grown in
132 Dulbecco's Modified Eagle's Medium, supplemented with 10 % inactivated Fetal Bovine Serum and
133 1 % penicillin in an incubator at 37 °C, 5 % CO₂ and saturating humidity. Following manufacturer
134 recommendations, cells were seeded at a concentration of 4×10³ cells/cm² in 96-well plates. After
135 48 h, cells were observed under phase contrast microscopy (Olympus, Japan) to ensure a confluence
136 between 70 to 80%. Subsequently, medium was absorbed and replenished with fresh medium
137 containing different concentrations of the PM extracts (500, 100, 50, 10, 5, 1, 0.5 and 0.1 µg/mL).
138 Four replicates were used for every concentration, including negative controls. After PM

139 application, cells were left in contact with the medium containing the particles during 72 h.

140 After exposure, the MTT reagent was added to the wells to a final concentration of 5 %. The wells
141 were incubated for 4 h until purple precipitate was visible. Subsequently, detergent was added to a
142 final concentration of 50 % (v/v) and samples were left in the dark for 2 h. Absorbance was then
143 measured at 570 nm using an Epoch 2 microplate spectrophotometer (BioTek, USA). To ensure
144 reproducibility of the procedure, this experiment was done twice. LC₅ doses were calculated by
145 using a biphasic equation from the dose-response scatter plot using the software Dr. Fit (Di Veroli et
146 al., 2015).

147 *2.6. Exposure strategy and metabolite extraction*

148 Cells were seeded and grown in 4.2 cm² chamber slides under the same conditions described for the
149 cytotoxicity assay (i.e. 37 °C, 5 % CO₂, saturating humidity, and plating density of 4×10³ cells/cm²).
150 After 48 h of cell proliferation, medium was extracted, and cells were exposed to media containing,
151 depending on the experiment, LC₅ or real dose of PM_{2.5-0.25} and PM_{0.25}. Chamber slides were
152 randomized for three exposure conditions: PM_{2.5-0.25}, PM_{0.25} and control. Six replicates were done
153 for every condition. Three independent experiments were conducted: one experiment, where the
154 real dose was applied and two experiments where the LC₅ was used. (Further information regarding
155 concentrations applied in each experiment can be seen in Table S1).

156 To extract the metabolites, we followed procedures previously published (Cuykx et al., 2017a,
157 2017b). In brief, after 72 h exposure, cells were washed twice with Phosphate Buffered Saline
158 (PBS) and cell metabolism was quenched by submerging cells into liquid nitrogen. Chamber slides
159 were then scraped three times with 200 µL of 80 % (v/v) MeOH/MilliQ-water and the content was
160 transferred to a vial containing 420 µL of chloroform and 500 µL of milliQ-water, having a final
161 solvent ratio of 2/3/2 water/MeOH/CHCl₃. The vials were then spiked with internal standards: 200
162 ng cholesterol-d₄, and 100 ng 2-ethylhexyl phosphate (TEHP) and lauric acid-d₃ for non-polar
163 fraction, and 200 ng tryptophane-d₅ and succinic acid-d₄ for the polar fraction. Vials were then

164 vortexed three times for 30 s, and equilibrated for 10 min at 4 °C. Subsequently they were
165 centrifuged at 3500 rpm during 7 min. The polar supernatant was transferred to pre-cooled
166 Eppendorf tubes, while the lower, non-polar phase was transferred to vials containing chloroform.
167 40 µL of polar phase from each sample were put in two Eppendorfs to make a couple of quality
168 control (QC) pools for polar compounds. Similarly, 20 µL of non-polar phase from each sample
169 were aggregated into two vials to obtain two QC non-polar pools. Samples and QC were evaporated
170 with nitrogen (non-polar phase) or using a centrifugal evaporator for 2.5 h (polar phase). Both, polar
171 and non-polar samples were stored at -80 °C prior to analysis.

172 2.7. *Metabolomics Set-up:*

173 Detail of the methods here employed can be consulted in Supplementary Materials. In brief, non-
174 polar vials and polar Eppendorfs were divided into two subsamples: one was positively ionized and
175 the other one was negatively ionized. This ionization methodology has proven to be successful for
176 metabolomic studies, given the heterogeneity and complexity of biological samples (Nordström et
177 al., 2008) Positive and negative non-polar vials were analyzed on a Kinetex XB-C18 (150 × 2.1 mm;
178 1.7 µm particle size, Phenomenex, Utrecht, the Netherlands). A mixture of MeOH, IPA, and NH₄Ac
179 (pH 6.7) was used as mobile phase in negative ionization mode, while a mixture of ACN, IPA, and
180 water with an acetate buffer (pH 4.2) was used as mobile phase in positive ionization mode.
181 Positive polar Eppendorfs were analyzed using an iHILIC column (100 × 2.1 mm; 1.8 µm particle
182 size, HILICON, Umea, Sweden) using ACN/MeOH and water with a NH₄F/FA buffer (pH 3.15) as
183 mobile phase. Negative polar Eppendorfs were analyzed through a Gemini[®] Phenyl-hexyl column
184 (150 × 2 mm, 3 µm particle size) (Phenomenex[®], Torrance, CA, USA). Mobile phase was a mixture
185 of MeOH, TBA and FA in MeOH/MilliQ water (pH=9). The columns were attached on an Agilent
186 Infinity 1290 UPLC (Agilent Technologies, Santa Clara, USA), and the detection was performed in an
187 Agilent 6530 QTOF with an Agilent Jet Stream nebulizer (Agilent Technologies).

188 2.8. *Data treatment:*

189 Mass-Hunter qualitative software (version 2.06.00, Agilent technologies) was used to evaluate LC
190 and MS parameters. To extract internal standards from the chromatogram, the “Find by Formula”-
191 algorithm (FBF) was used. Deconvolution algorithm was set to retain peaks having a quality score
192 higher than 80% and abundance greater than 3000. These signals were subsequently grouped into
193 molecular features according to their m/z, retention time, and correspondence to isotopes or
194 adducts. Extracted features represent thus the different m/z signals of a metabolite. Mass Profiler
195 (v12.5, Agilent Technologies, Santa Clara, CA, USA) was used to merge data coming from
196 consecutive runs. The sums of the areas of all ions of the molecular features were the dependent
197 values of the variables.

198 Features present in at least 80 % of the samples were retained for statistical analysis. This analysis
199 was performed using the software EZ info v 2.0 (Umetrics, Umeå, Sweden). Principal Component
200 Analysis (PCA) and Orthogonal Partial Least Squares-Discriminant Analysis (OPLS-DA)
201 techniques were applied to estimate the quality of the dataset and to detect molecular features of
202 interest respectively. Welch T tests with Benjamini-Hochberg correction were used to evaluate the
203 significance of differences of PM levels among environments, PM fractions (cytotoxicity), and
204 between exposed and control groups (metabolomic assays). Those differences were considered
205 significant when the corrected p was below 0.05.

206 Annotation of significant features was performed using Molecular Formula Generator algorithm
207 from the Mass-Hunter software. Tentative formulas were calculated having into account a mass
208 error of 10 ppm, isotope spacing of 5 ppm, and a maximal 5 % difference in abundance compared to
209 the calculated isotopic pattern. To find structures for these features, a search was performed in
210 LipidMaps, Metlin, and Human Metabolome Database (HMDB) (Fahy et al., 2007; Smith et al.,
211 2005; Wishart et al., 2013). The levels of confidence in identification are reported according to
212 Schymanski et al. (2014). Heat maps were designed using the online resource Metaboanalyst v 4.0
213 (Xia and Wishart, 2016).

214

215 3. Results and discussion

216 3.1. PM levels and time activity pattern:

217 Concentrations of the three PM fractions measured in the different microenvironments can be seen
218 on Figure 1.

219 Sensitivity in our samples was $0.39 \mu\text{g}/\text{m}^3$, which introduces an uncertainty between 10 and 20% in
220 $\text{PM}_{2.5-0.25}$ at home and outdoors. Average outdoor values obtained in this study were within the
221 range of the average annual values reported by the Catalonian Administration during the last five
222 years in the same area (Generalitat de Catalunya, 2017). Although not statistically significant,
223 ($p>0.05$), average outdoor concentrations were higher than those registered during the same days by
224 the air quality monitor stations in the area (16.6 and $9.3 \mu\text{g}/\text{m}^3$ for PM_{10} and $\text{PM}_{2.5}$ respectively)
225 (Generalitat de Catalunya, 2016). Average PM concentrations were below the thresholds set by the
226 European legislation (i.e. daily average of $50 \mu\text{g}/\text{m}^3$ for PM_{10} , and annual average of $40 \mu\text{g}/\text{m}^3$ and
227 $25 \mu\text{g}/\text{m}^3$ for PM_{10} and $\text{PM}_{2.5}$ respectively) (European Commission and EU Parliament, 2008). The
228 highest concentrations for every PM fraction were observed in classrooms, while the levels at home
229 were the lowest. These results could be highly related with the occupancy of these
230 microenvironments. The higher the human activity, the greater the resuspension and contribution of
231 organic PM (textile fibers and skin debris) indoors (Serfozo et al., 2014; Viana et al., 2014). The
232 low occupancy at home, in combination with the lack of ventilation and absence of other indoor
233 sources in the room (i.e. tobacco, gas stove), could be the cause of experiencing lower PM levels at
234 home than outdoors. This same trend has been reported previously for dwellings having similar
235 characteristics to the one used in this study (Romagnoli et al., 2016; Xiao et al., 2018).

236 Regarding time activity patterns, share of time spent by students in the different microenvironments
237 and performing the different activities can be seen on Figure 2:

238 Kids spent most of their time (90 %) indoors, while the outdoor time was mostly used during heavy
239 intensity activities. The most time-demanding activity was sleeping (9.5 hours per day), while same

240 share of time was spent sitting in school and at home (5 hours each activity). Light exercise at home
241 was performed for 2 hours a day, while only half an hour of light exercise outdoors was reported.
242 Heavy exercise was fully performed outdoors, spending a daily average of 2 hours for this activity.
243 The activity pattern obtained in the present study were similar to those obtained by other
244 researchers in western countries (Cohen Hubal et al., 2000; Matz et al., 2015).

3.2. Deposition pattern of particles and real dose calculation

245 Daily deposited mass of the three sampled PM fractions can be seen on Table 1. The PM fraction
246 registering the highest overall deposition masses was $PM_{10-2.5}$. This fraction was mostly deposited
247 in the head and tracheobronchial regions of the respiratory tract, while, as seen in previous studies,
248 the amount of coarse particles reaching the lung was minor (Sánchez-Soberón et al., 2015). Despite
249 the scarce amount of time spent outdoors performing high intensity activities (2 hours per day), this
250 activity reached the highest share of PM deposition regardless PM fraction. Fine fractions ($PM_{2.5-0.25}$
251 and $PM_{0.25}$), however, followed a different deposition pattern within the respiratory tract. Between
252 30 and 40 % of the total deposited mass of these fractions was addressed in the lung. Deposited
253 mass of $PM_{2.5-0.25}$ in lungs reaches its maximum during class time. In the case of $PM_{0.25}$, heavy
254 exercise outdoors is the activity registering the highest deposition masses for every respiratory
255 region. Regardless of PM fraction studied, head region registered the highest deposition masses.

256 These variances in deposition patterns of the three PM fractions are related to the different levels of
257 PM experienced in every environment, but also by the deposition mechanisms considered in the
258 MPPD model: inertial impaction, sedimentation (gravitational setting), and diffusion (Brown et al.,
259 2013). Impaction and sedimentation are the dominant mechanisms in particles bigger than $1 \mu m$
260 (Salma et al., 2015). These mechanisms are highly dependent on the air speed on the respiratory
261 tract (Hussain et al., 2011). Thus, high air speeds will favor the impaction, while low velocities will
262 favor sedimentation. Furthermore, the larger the PM, the more likely is to experience one of these
263 processes. Diffusion mechanism appears in particles smaller than $0.5 \mu m$, which behave like gas
264 molecules. Particles within this size follow a Brownian motion, and they deposit at random (Bakand

265 et al., 2012).

266 In the first part of the respiratory tract, the speed of inhaled air reaches the highest velocity within
267 the respiratory tract. Furthermore, as soon as the activity intensity increases, so does the air velocity.
268 Consequently, impaction phenomenon is the dominant deposition mechanism in head region,
269 affecting especially those particles of bigger size during high intensity activities (Hussain et al.,
270 2011). Air passing through the tracheobronchial region experiences a deceleration, causing the
271 sedimentation of the heaviest particles. When reaching terminal areas of the respiratory tract, the
272 speed of air is minimal, which favors sedimentation. However, at this point, most of the coarse PM
273 has been already deposited, and diffusion mechanism of $PM_{0.25}$ becomes the most important
274 deposition process (CCOHS, 2010).

275 Based on these results, the amount of $PM_{2.5-0.25}$ and $PM_{0.25}$ deposited into the pulmonary region
276 after 72 h would be 30.75 and 80.11 μg , respectively. To perform *in vitro* toxicity studies, the doses
277 were converted to 0.27 ng/mL and 0.70 ng/mL of $PM_{2.5-0.25}$ and $PM_{0.25}$, respectively (Table S1).

278 3.3. Cytotoxicity

279 Since the mass of $PM_{10-2.5}$ reaching the lungs was negligible, toxicity assays were performed for
280 $PM_{2.5-0.25}$ and $PM_{0.25}$. As reported in previous studies using same cell line and PM fractions,
281 internalization of PM was reported in our cells (Figure S2)(Dominici et al., 2013). Dose-response
282 plot graphs, as well as fitting equations for both PM fractions can be seen in Figure 3. Biphasic
283 decay was the best fitting equation for our data, so it was chosen to calculate the concentration
284 corresponding to 5% of mortality (LC_5). The smaller PM fraction causes a higher toxicity,
285 especially when applying doses ranging from 0.5 to 10 $\mu\text{g/mL}$. Consequently, estimated LC_5 for
286 $PM_{0.25}$ was lower than for $PM_{2.5-0.25}$ (8.08 ng/mL and 73.70 ng/mL respectively). It should be noted
287 that in our case, these LC_5 values are out of the ranges of concentrations assessed in our cytotoxicity
288 assay. Subsequent microscopic observations of cells after the use of these doses were performed,
289 corroborating a slightly higher cell mortality than control cells, which is appropriate to perform

290 metabolomic assays. However, these values are an approach to real LC_5 , and should not be taken as
291 absolute values for this indicator. This trend of a higher toxicity of smaller PM has been reported
292 before (L. Cao et al., 2015; Guan et al., 2016; Zou et al., 2017). In fact, this reduction in the size is
293 related with a greater surface area, which can, apart from chemical composition, induce higher
294 damage to cells (Kelly and Fussell, 2012).

295 Comparing our result with previous research is complicated. Few studies have been developed to
296 evaluate the cytotoxicity of A549 cells after 72 h exposure to PM, and to our best knowledge, none
297 of them has divided $PM_{2.5}$ into two fractions. Ho et al. (2016) obtained similar toxicity values (i.e.
298 LC_{50}) after exposing A549 cells to $PM_{2.5}$ from coal burning origin. However, other studies using
299 environmental or household $PM_{2.5}$ reported higher LC_{50} values (M. Huang et al., 2015; Q. Huang et
300 al., 2015). Apart from differences in the PM fractions here assessed, differences between studies
301 could be the result of different PM chemical composition and shape (data of these parameters for
302 the present study is in preparation). Other factor influencing differences among studies is the
303 diverse methodologies used in the above cited studies. Particulate matter collection media varies
304 from fiber filters to PTFE membranes, and extraction of PM has been performed under ultrapure
305 water or methanol. In the present study we decided to use PC filters for both, their ease in PM
306 extraction without excessive mechanical means, and their hydrophilicity (Greenwell et al., 2002).
307 This make them suitable to obtain PM aqueous solutions, as expected to find inside the lungs (Cross
308 et al., 1994).

309 3.4. Metabolomics:

310 Regardless of experiment performed, between 1400 and 1600 non-polar features, and between 1100
311 and 1400 polar features per replicate were detected in the present study. These numbers are in line
312 with the performance reported previously using the same methodology (Cuykx et al., 2017b).

313 3.4.1. LC_5 experiment:

314 After analyzing metabolic changes in exposed cells, those replicates treated with $PM_{0.25}$ LC_5

315 presented significant differences in the content of 39 metabolites compared to control cells (Tables
316 S2 and S3). On the other hand, cells exposed to $PM_{2.5-0.25}$ LC₅ showed significant differences in the
317 content of 38 features with respect to control replicates (Tables S4, and S5).

318 Hierarchical clustering analysis of these features, as well as the samples, can be seen in Figure 4.
319 According to this heat map, there is a grouping of samples into two marked groups: exposed and
320 control. At the same time, there are a couple of clusters within the exposed group: one exclusively
321 formed by 5 $PM_{0.25}$ replicates (green color dashed square), and the other comprising $PM_{2.5-0.25}$ and
322 the remaining $PM_{0.25}$ replicate (blue color dashed line). This last $PM_{0.25}$ replicate showed a
323 metabolic profile (i.e. fold change values in the altered metabolites) closer to the overall metabolic
324 profile displayed by cell exposed to $PM_{2.5-0.25}$. Regarding compounds, a disposition into two groups
325 was noted depending on the overall regulation pattern. The first group (yellow dot-dashed square)
326 contains mostly downregulated features in exposed cells, which comprised cardiolipins (CLs),
327 phosphatidylserines (PSs), and most of phosphatidylcholines (PCs). The second group (purple dot-
328 dashed square) is mainly formed by the upregulated features and includes all identified ceramides
329 (CERs).

330 Regardless of PM fraction applied, most of the altered metabolites were non-polar (Tables S2 and
331 S3). The vast majority of them were triglycerides (TG), CERs, and phospholipids. More
332 specifically, these changes have been detected for PSs, PCs, PEs, and CLs. These metabolites are
333 important constituents of cells membranes (Stillwell, 2016). Triglycerides and PCs are also the main
334 components of lung surfactant, a protein-lipid mixture essential to reduce tension at the alveoli air-
335 liquid interphase (Bernhard et al., 2001; Lopez-Rodriguez and Pérez-Gil, 2014).

336 Under normal conditions, PSs are located in the inner part of the plasma membrane. But in cells
337 undergoing the apoptosis process, these lipids turn to the external surface of the cell membrane,
338 sending a distress signal to macrophages in order to be phagocyted (Segawa and Nagata, 2015).
339 Consequently, these substances have been studied as biomarkers of different diseases, such as
340 cancer (Sharma and Kanwar, 2017). Although we were not able to locate where in the cell

341 membrane PSs were, we noticed a downregulation of this group of compounds in both ($PM_{2.5-0.25}$
342 and $PM_{0.25}$) exposed groups.

343 Phosphatidylethanolamines (PEs) play a significant role in membrane fusion and division,
344 apoptosis, and autophagy (Pavlovic and Bakovic, 2013). Our results show significant
345 downregulation in the content of most PEs regardless of PM fraction applied. Phosphatidylcholines
346 (PCs), are the main component of lung surfactant (Bernhard et al., 2001). Cells exposed to $PM_{0.25}$
347 showed an overall upregulation in PC content, while those cells exposed to $PM_{2.5-0.25}$ showed an
348 overall downregulation. This size related response in PC regulation has been previously reported in
349 other studies (Chen et al., 2014; Juvin et al., 2002; Wang et al., 2017).

350 PCs and PEs are mainly generated via a couple of mechanisms (Figure 5): *de novo* or from PS
351 decarboxylation (Bleijerveld et al., 2007; Vance, 2008). In *de-novo* pathway, PEs and PCs are
352 generated from ethanolamine and choline, respectively. (Gibellini and Smith, 2010). The other
353 pathway consists on the transformation of PS to PE via decarboxylation. This PE can be then
354 transformed into PC by the action of phosphatidyl-ethanolamine N-methyltransferase (PEMT)
355 (Zinrajh et al., 2014).

356 $PM_{2.5-0.25}$ elicits an overall downregulation on PSs, PEs, and PCs (Figure 5a). In mammalian cells,
357 PSs are synthesized exclusively from PEs and PCs (Vance and Tasseva, 2013). Therefore, a decrease
358 in the synthesis of PEs and PCs will lead to a decrease on PCs. Thus, $PM_{2.5-0.25}$ could be affecting
359 the *de novo* pathway. On the other hand, $PM_{0.25}$ are more likely to affect the PS decarboxylation
360 pathway, increasing the levels of PCs by transforming PSs to PEs, and PEs into PCs (Figure 5b).
361 These differences in the way of action between $PM_{2.5-0.25}$ and $PM_{0.25}$ could be due to differences in
362 physicochemical characteristics between these two fractions.

363 A downregulation in CLs was significant in this study, regardless of the PM fraction exposed. CLs
364 are almost exclusively localized in the inner mitochondrial membrane (Houtkooper and Vaz, 2008).
365 Cardiolipins improve the ATP generation via oxidative phosphorylation within this organelle, apart

366 from being involved in other mitochondrial processes (Claypool and Koehler, 2012). , and more
367 specifically, its polar toxic constituents have been recognized previously as disruptors of
368 mitochondrial functions (Xia et al., 2004). Although using different kind of cells, Hiura et al. (2000)
369 also recorded a decrease in mitochondrial CLs after exposing mice macrophages to PM. This
370 damage in the mitochondrial membrane could be generated by the particle surface (mechanical
371 damage), or by formation of reactive oxygen species (ROS) (von Moos and Slaveykova, 2014).

372 Ceramides are highly concentrated in cell membranes and play a significant role in the response to
373 stress stimuli (Bikman and Summers, 2011). The upregulation of CERs is recognized as a signal of
374 apoptosis and has been related to several lung diseases (Lee et al., 2015; Petrache et al., 2005).
375 Previous studies reported clear upregulations of CERs after PM exposures (Peuschel et al., 2012;
376 Zhang et al., 2017). However, the regulations of these CERs were variable, and fold changes were
377 low. This difference could be explained by the PM doses applied in the present study, which were
378 lower than the previously reported papers.

379 Regarding polar constituents (Tables S4 and S5), cells exposed to $PM_{2.5-0.25}$ showed an upregulation
380 in N1-Acetylspermidine, a precursor of spermidine (Wishart et al., 2013). Spermidine is involved in
381 regulation of inflammatory reactions, and has been recognized as defense line against reactive
382 oxygen species and DNA protector in lungs (Hoet and Nemery, 2000). On the other hand, cells
383 exposed to $PM_{0.25}$ showed and upregulation in 1-Pyrroline-5-carboxylic acid. This compound is a
384 precursor, of L-proline, which is able to generate specific reactive oxygen species (ROS) acting as
385 signals for tumor suppression, apoptosis and cell survival (Liang et al., 2013; Wishart et al., 2013).
386 Furthermore, proline metabolism can be used as a source of energy under stress conditions within
387 cells (Phang et al., 2015).

388 3.4.2. *Real dose experiment*

389 When cells were exposed to realistic PM doses, the number of significant features had been reduced
390 to 10 for $PM_{0.25}$ and 5 for $PM_{2.5-0.25}$ (Tables S5 and S6). Under real conditions, $PM_{0.25}$ doses are

391 higher than $PM_{2.5-0.25}$, and consequently a higher effect of these particles to the cells could be
392 observed.

393 As shown in Figure 6, hierarchical grouping of replicates is not as clear as during the LC_5 exposure.
394 Replicates are distributed into two groups: the first comprising exposed cells of both PM fractions,
395 while the second comprises a mix of exposed and control cells. Nevertheless, a plausible tendency
396 in sample distribution can be drawn: exposure to PM tend to cluster in comparison to control
397 samples. There is also a grouping in compounds: in a first group it is possible to differentiate those
398 features upregulated in the exposed cells (yellow dot-dashed square), while the second group
399 comprises those compounds showing fold changes dependent on the used PM (purple dot-dashed
400 square).

401 Contrary to the LC_5 experiment, the number of affected features after $PM_{0.25}$ exposure was higher
402 for polar (7) than for non-polar (3), which could reveal less intensive effects on cell membranes.
403 Cells exposed to $PM_{0.25}$ experienced an upregulation in the content of most altered metabolites,
404 such as proline, TGs, and PEs. These results could indicate that cells are undergoing a hormesis
405 phase, in which cells are activated as a consequence of being exposed to low doses of toxic agents
406 (Zimmermann et al., 2014). Cells exposed to $PM_{2.5-0.25}$ showed an overall decrease in the altered
407 metabolites. Slight downregulations were noticed for PEs and phosphatidylglycerols (PGs), one of
408 the constituents of lung surfactant and also present at small scale in cell membranes (Stillwell,
409 2016). However, as previously pointed out, the number of altered metabolites in this experiment
410 was small, showing a higher fold change variability among the same exposure group replicates.

411 Despite the promising results of the approach here described, this study still presents some
412 limitations that should be faced in future studies. First, the number of students surveyed, the number
413 of environments assessed, and sampling duration should be increased to obtain wider conclusions.
414 Uncertainty in $PM_{2.5-0.25}$ levels should be decreased by either, increasing sampling time or using a
415 more sensitive balance. Regarding *in-vitro* assays, a more accurate calculation of LC_5 is needed, as
416 pointed out previously. Also, having access to a PM-controlled air chamber would be useful to

417 obtain more appropriate negative controls. Finally, to simplify dosage strategy, real doses were
418 calculated having into account the total surface of the culture dishes, instead of the percentage of
419 cell confluence.

420 **4. Conclusions**

421 Three fractions of PM ($PM_{0.25}$, $PM_{2.5-0.25}$, and $PM_{10-2.5}$) were collected in three environments
422 (outdoor, classroom, and home) within a village located nearby an industrial complex. The time
423 activity patterns of 20 students attending school were obtained to study the exposure and deposition
424 of PM within the children's respiratory tract. Afterwards, these particles were extracted from filters
425 and put in contact with alveolar A549 cells to study the cytotoxicity and changes in the metabolic
426 profile after 72 h exposure. Classroom microenvironment registered the highest levels of every PM
427 fraction collected, due to its higher occupancy. Regardless of PM fraction, the upper respiratory
428 tract (head) was the region that retained most of the overall deposited mass, especially when
429 performing heavy intensity activities. The finest fraction ($PM_{0.25}$) elicited a higher cytotoxicity than
430 $PM_{2.5-0.25}$. The number of metabolites affected by particles exposure was similar for both fractions
431 in LC_5 doses, while after applying real doses changes were mainly due to $PM_{0.25}$. These changes
432 were mostly in compounds dealing with cell and mitochondrial membrane functions, revealing the
433 potential of PM to elicit both extracellular and intracellular damage.

434 **Acknowledgments**

435 This study was financed by the Spanish Ministry of Economy and Competitiveness (MINECO) as
436 part of the project CTM2015-65303-P. Francisco Sánchez-Soberón received a doctoral scholarship
437 and an internship grant from the same organism.

438 **References**

439 ARA, 2014. ARA :: Products :: MPPD [WWW Document]. URL

440 <http://www.ara.com/products/mppd.htm> (accessed 8.24.15).

441 Bakand, S., Hayes, A., Dechsakulthorn, F., 2012. Nanoparticles: a review of particle toxicology

- 442 following inhalation exposure. *Inhal. Toxicol.* 24, 125–135.
- 443 Bernhard, W., Hoffmann, S., Dombrowsky, H., Rau, G.A., Kamlage, A., Kappler, M., Haitzma, J.J.,
444 Freihorst, J., von der Hardt, H., Poets, C.F., 2001. Phosphatidylcholine Molecular Species in
445 Lung Surfactant. *Am. J. Respir. Cell Mol. Biol.* 25, 725–731. doi:10.1165/ajrcmb.25.6.4616
- 446 Bikman, B.T., Summers, S.A., 2011. Ceramides as modulators of cellular and whole-body
447 metabolism. *J. Clin. Invest.* doi:10.1172/JCI57144
- 448 Bleijerveld, O.B., Brouwers, J.F.H.M., Vaandrager, A.B., Helms, J.B., Houweling, M., 2007. The
449 CDP-ethanolamine Pathway and Phosphatidylserine Decarboxylation Generate Different
450 Phosphatidylethanolamine Molecular Species. *J. Biol. Chem.* 282, 28362–28372.
451 doi:10.1074/jbc.M703786200
- 452 Brown, J.S., Gordon, T., Price, O., Asgharian, B., 2013. Thoracic and respirable particle definitions
453 for human health risk assessment. Part. *Fibre Toxicol.* 10, 12. doi:10.1186/1743-8977-10-12
- 454 Cao, L., Zeng, J., Liu, K., Bao, L., Li, Y., 2015. Characterization and Cytotoxicity of PM_{<0.2},
455 PM_{0.2–2.5} and PM_{2.5–10} around MSWI in Shanghai, China. *Int. J. Environ. Res. Public*
456 *Health* 12, 5076–5089. doi:10.3390/ijerph120505076
- 457 Cao, X., Lin, H., Muskhelishvili, L., Latendresse, J., Richter, P., Heflich, R.H., 2015. Tight junction
458 disruption by cadmium in an in vitro human airway tissue model. *Respir. Res.* 16, 30.
459 doi:10.1186/s12931-015-0191-9
- 460 CCOHS, 2010. How Do Particulates Enter the Respiratory System? [WWW Document]. *Can. Cent.*
461 *Occup. Heal. Saf.* URL https://www.ccohs.ca/oshanswers/chemicals/how_do.html (accessed
462 1.4.18).
- 463 Chen, M., Li, B., Sang, N., 2017. Particulate matter (PM_{2.5}) exposure season-dependently induces
464 neuronal apoptosis and synaptic injuries. *J. Environ. Sci. (China)* 54, 336–345.
465 doi:10.1016/j.jes.2016.10.013
- 466 Chen, W.-L., Lin, C.-Y., Yan, Y.-H., Cheng, K.T., Cheng, T.-J., 2014. Alterations in rat pulmonary
467 phosphatidylcholines after chronic exposure to ambient fine particulate matter. *Mol. BioSyst.*

- 468 10, 3163–3169. doi:10.1039/C4MB00435C
- 469 Claypool, S.M., Koehler, C.M., 2012. The complexity of cardiolipin in health and disease. Trends
470 Biochem. Sci. 37, 32–41. doi:10.1016/j.tibs.2011.09.003
- 471 Cohen Hubal, E.A., Sheldon, L.S., Burke, J.M., McCurdy, T.R., Berry, M.R., Rigas, M.L.,
472 Zartarian, V.G., Freeman, N.C., 2000. Children’s exposure assessment: a review of factors
473 influencing Children’s exposure, and the data available to characterize and assess that
474 exposure. Environ. Health Perspect. 108, 475–486.
- 475 Cross, C.E., van der Vliet, A., O’Neill, C.A., Louie, S., Halliwell, B., 1994. Oxidants, antioxidants,
476 and respiratory tract lining fluids. Environ. Health Perspect. 185–91.
- 477 Cuykx, M., Mortelé, O., Rodrigues, R.M., Vanhaecke, T., Covaci, A., 2017a. Optimisation of in
478 vitro sample preparation for LC-MS metabolomics applications on HepaRG cell cultures.
479 Anal. Methods 9, 3704–3712. doi:10.1039/C7AY00573C
- 480 Cuykx, M., Negreira, N., Beirnaert, C., Van den Eede, N., Rodrigues, R., Vanhaecke, T., Laukens,
481 K., Covaci, A., 2017b. Tailored liquid chromatography–mass spectrometry analysis improves
482 the coverage of the intracellular metabolome of HepaRG cells. J. Chromatogr. A 1487, 168–
483 178. doi:10.1016/j.chroma.2017.01.050
- 484 Di Veroli, G.Y., Fornari, C., Goldlust, I., Mills, G., Koh, S.B., Bramhall, J.L., Richards, F.M.,
485 Jodrell, D.I., 2015. An automated fitting procedure and software for dose-response curves with
486 multiphasic features. Sci. Rep. 5, 14701. doi:10.1038/srep14701
- 487 Dominici, L., Guerrero, E., Villarini, M., Fatigoni, C., Moretti, M., Blasi, P., Monarca, S., 2013.
488 Evaluation of in vitro cytotoxicity and genotoxicity of size-fractionated air particles sampled
489 during road tunnel construction. Biomed Res. Int. 2013, 1–9. doi:10.1155/2013/345724
- 490 Donahue, N.M., Posner, L.N., Westervelt, D.M., Li, Z., Shrivastava, M., Presto, A.A., Sullivan,
491 R.C., Adams, P.J., Pandis, S.N., Robinson, A.L., Donahue, N.M., Posner, L.N., Westervelt,
492 D.M., Li, Z., Shrivastava, M., Presto, A.A., Sullivan, R.C., Adams, P.J., Pandis, S.N.,
493 Robinson, A.L., 2016. Where Did This Particle Come From? Sources of Particle Number and

- 494 Mass for Human Exposure Estimates, in: Hester, R.E., Harrison, R.M., Querol, X. (Eds.),
495 Airborne Particulate Matter: Sources, Atmospheric Processes and Health. pp. 35–71.
496 doi:10.1039/9781782626589-00035
- 497 Dunnill, M.S., 1962. Postnatal Growth of the Lung. *Thorax* 17, 329–333. doi:10.1136/thx.17.4.329
- 498 European Commission, EU Parliament, 2008. Directive 2008/50/EC of the European Parliament
499 and of the Council of 21 May 2008 on ambient air quality and cleaner air for Europe. *Off. J.*
500 *Eur. Communities.* 152, 1–44.
- 501 Fahy, E., Sud, M., Cotter, D., Subramaniam, S., 2007. LIPID MAPS online tools for lipid research.
502 *Nucleic Acids Res.* 35, W606-12. doi:10.1093/nar/gkm324
- 503 Generalitat de Catalunya, 2017. La qualitat de l'aire a Catalunya [WWW Document]. URL
504 <http://www.qualitatdelaire.cat/contaminant/cerca/7/4/14.html> (accessed 6.4.18).
- 505 Generalitat de Catalunya, 2016. Dades de qualitat de l'aire v 1.2.8 [WWW Document]. URL
506 <http://dtes.gencat.cat/icqa/> (accessed 6.4.18).
- 507 Gibellini, F., Smith, T.K., 2010. The Kennedy pathway-De novo synthesis of
508 phosphatidylethanolamine and phosphatidylcholine. *IUBMB Life* 62, n/a-n/a.
509 doi:10.1002/iub.337
- 510 Greenwell, L.L., Jones, T.P., Richards, R.J., 2002. The collection of PM10 for toxicological
511 investigation: Comparisons between different collecting devices. *Environ. Monit. Assess.* 79,
512 251–273. doi:10.1023/A:1020230727359
- 513 Guan, L., Rui, W., Bai, R., Zhang, W., Zhang, F., Ding, W., 2016. Effects of Size-Fractionated
514 Particulate Matter on Cellular Oxidant Radical Generation in Human Bronchial Epithelial
515 BEAS-2B Cells. *Int. J. Environ. Res. Public Health* 13, 483. doi:10.3390/ijerph13050483
- 516 Hiura, T.S., Li, N., Kaplan, R., Horwitz, M., Seagrave, J.-C., Nel, A.E., 2000. The Role of a
517 Mitochondrial Pathway in the Induction of Apoptosis by Chemicals Extracted from Diesel
518 Exhaust Particles. *J. Immunol.* 165, 2703–2711. doi:10.4049/jimmunol.165.5.2703
- 519 Ho, K.F., Chang, C.C., Tian, L., Chan, C.S., Musa Bandowe, B.A., Lui, K.H., Lee, K.Y., Chuang,

- 520 K.J., Liu, C.Y., Ning, Z., Chuang, H.C., 2016. Effects of polycyclic aromatic compounds in
521 fine particulate matter generated from household coal combustion on response to EGFR
522 mutations in vitro. *Environ. Pollut.* 218, 1262–1269. doi:10.1016/j.envpol.2016.08.084
- 523 Hoet, P.H., Nemery, B., 2000. Polyamines in the lung: polyamine uptake and polyamine-linked
524 pathological or toxicological conditions. *Am. J. Physiol. Lung Cell. Mol. Physiol.* 278, L417-
525 33.
- 526 Horgan, R.P., Kenny, L.C., 2011. “Omic” technologies: genomics, transcriptomics, proteomics and
527 metabolomics. *Obstet. Gynaecol.* 13, 189–195. doi:10.1576/toag.13.3.189.27672
- 528 Houtkooper, R.H., Vaz, F.M., 2008. Cardiolipin, the heart of mitochondrial metabolism. *Cell. Mol.*
529 *Life Sci.* 65, 2493–2506. doi:10.1007/s00018-008-8030-5
- 530 Huang, M., Kang, Y., Wang, W., Chan, C.Y., Wang, X., Wong, M.H., 2015. Potential cytotoxicity of
531 water-soluble fraction of dust and particulate matters and relation to metal(loid)s based on
532 three human cell lines. *Chemosphere* 135, 61–66. doi:10.1016/j.chemosphere.2015.04.004
- 533 Huang, Q., Zhang, J., Luo, L., Wang, X., Wang, X., Alamdar, A., Peng, S., Liu, L., Tian, M., Shen,
534 H., 2015. Metabolomics reveals disturbed metabolic pathways in human lung epithelial cells
535 exposed to airborne fine particulate matter. *Toxicol. Res.* 4, 939–947.
536 doi:10.1039/C5TX00003C
- 537 Hussain, M., Madl, P., Khan, A., 2011. Lung deposition predictions of airborne particles and the
538 emergence of contemporary diseases, Part-I. *Health (Irvine. Calif.)* 2, 51–59.
- 539 Juvin, P., Fournier, T., Grandsaigne, M., Desmots, J.-M., Aubier, M., 2002. Diesel particles
540 increase phosphatidylcholine release through a NO pathway in alveolar type II cells. *Am. J.*
541 *Physiol. - Lung Cell. Mol. Physiol.* 282, L1075–L1081. doi:10.1152/ajplung.00213.2001
- 542 Kelly, F., Fussell, J., 2016. Health Effects of Airborne Particles in Relation to Composition, Size
543 and Source, in: *Airborne Particulate Matter: Sources, Atmospheric Processes and Health*. pp.
544 344–372.
- 545 Kelly, F.J., Fussell, J.C., 2012. Size, source and chemical composition as determinants of toxicity

- 546 attributable to ambient particulate matter. *Atmos. Environ.* 60, 504–526.
547 doi:10.1016/j.atmosenv.2012.06.039
- 548 Lee, J., Yeganeh, B., Ermini, L., Post, M., 2015. Sphingolipids as cell fate regulators in lung
549 development and disease. *Apoptosis* 20, 740–757. doi:10.1007/s10495-015-1112-6
- 550 Liang, X., Zhang, L., Natarajan, S.K., Becker, D.F., 2013. Proline mechanisms of stress survival.
551 *Antioxid. Redox Signal.* 19, 998–1011. doi:10.1089/ars.2012.5074
- 552 Líbalová, H., Uhlířová, K., Kléma, J., Machala, M., Šrám, R.J., Ciganek, M., Topinka, J., 2012.
553 Global gene expression changes in human embryonic lung fibroblasts induced by organic
554 extracts from respirable air particles. Part. *Fibre Toxicol.* 9, 1. doi:10.1186/1743-8977-9-1
- 555 Longhin, E., Capasso, L., Battaglia, C., Proverbio, M.C., Cosentino, C., Cifola, I., Mangano, E.,
556 Camatini, M., Gualtieri, M., 2016. Integrative transcriptomic and protein analysis of human
557 bronchial BEAS-2B exposed to seasonal urban particulate matter. *Environ. Pollut.* 209, 87–98.
558 doi:10.1016/j.envpol.2015.11.013
- 559 Lopez-Rodriguez, E., Pérez-Gil, J., 2014. Structure–function relationships in pulmonary surfactant
560 membranes: From biophysics to therapy. *Biochim. Biophys. Acta - Biomembr.* 1838, 1568–
561 1585. doi:10.1016/j.bbamem.2014.01.028
- 562 MAPAMA, 2018. Inventario de instalaciones - Inventario Completo [WWW Document]. URL
563 <http://www.prtr-es.es/Informes/InventarioInstalacionesIPPC.aspx> (accessed 2.19.18).
- 564 Matz, C.J., Stieb, D.M., Brion, O., 2015. Urban-rural differences in daily time-activity patterns,
565 occupational activity and housing characteristics. *Environ. Heal.* 14, 88. doi:10.1186/s12940-
566 015-0075-y
- 567 Megido, L., Suárez-Peña, B., Negral, L., Castrillón, L., Suárez, S., Fernández-Nava, Y., Marañón,
568 E., 2016. Relationship between physico-chemical characteristics and potential toxicity of
569 PM10. *Chemosphere* 162, 73–79. doi:10.1016/j.chemosphere.2016.07.067
- 570 Mesquita, S.R., Van Drooge, B.L., Oliveira, E., Grimalt, J.O., Barata, C., Vieira, N., Guimarães, L.,
571 Piña, B., 2015. Differential embryotoxicity of the organic pollutants in rural and urban air

- 572 particles. *Environ. Pollut.* 206, 535–542. doi:10.1016/j.envpol.2015.08.008
- 573 Nordström, A., Want, E., Northen, T., Lehtiö, J., Siuzdak, G., 2008. Multiple Ionization Mass
574 Spectrometry Strategy Used To Reveal the Complexity of Metabolomics. *Anal. Chem.* 80,
575 421–429. doi:10.1021/ac701982e
- 576 Pavlovic, Z., Bakovic, M., 2013. Regulation of Phosphatidylethanolamine Homeostasis—The
577 Critical Role of CTP:Phosphoethanolamine Cytidylyltransferase (Pcvt2). *Int. J. Mol. Sci.* 14,
578 2529–50. doi:10.3390/ijms14022529
- 579 Peixoto, M.S., de Oliveira Galvão, M.F., Batistuzzo de Medeiros, S.R., 2017. Cell death pathways
580 of particulate matter toxicity. *Chemosphere.* doi:10.1016/j.chemosphere.2017.08.076
- 581 Petrache, I., Natarajan, V., Zhen, L., Medler, T.R., Richter, A.T., Cho, C., Hubbard, W.C.,
582 Berdyshev, E. V, Tuder, R.M., 2005. Ceramide upregulation causes pulmonary cell apoptosis
583 and emphysema-like disease in mice. *Nat. Med.* 11, 491–498. doi:10.1038/nm1238
- 584 Peuschel, H., Sydlik, U., Grether-Beck, S., Felsner, I., Stöckmann, D., Jakob, S., Kroker, M.,
585 Haendeler, J., Gotić, M., Bieschke, C., Krutmann, J., Unfried, K., 2012. Carbon nanoparticles
586 induce ceramide- and lipid raft-dependent signalling in lung epithelial cells: A target for a
587 preventive strategy against environmentally-induced lung inflammation. *Part. Fibre Toxicol.* 9,
588 48. doi:10.1186/1743-8977-9-48
- 589 Phang, J.M., Liu, W., Hancock, C.N., Fischer, J.W., 2015. Proline metabolism and cancer. *Curr.*
590 *Opin. Clin. Nutr. Metab. Care* 18, 71–77. doi:10.1097/MCO.0000000000000121
- 591 Roig, N., Sierra, J., Rovira, J., Schuhmacher, M., Domingo, J.L., Nadal, M., 2013. In vitro tests to
592 assess toxic effects of airborne PM(10) samples. Correlation with metals and chlorinated
593 dioxins and furans. *Sci. Total Environ.* 443, 791–797. doi:10.1016/j.scitotenv.2012.11.022
- 594 Romagnoli, P., Balducci, C., Perilli, M., Vichi, F., Imperiali, A., Cecinato, A., 2016. Indoor air
595 quality at life and work environments in Rome, Italy. *Environ. Sci. Pollut. Res.* 23, 3503–3516.
596 doi:10.1007/s11356-015-5558-4
- 597 Salma, I., Füre, P., Németh, Z., Balásházy, I., Hofmann, W., Farkas, Á., 2015. Lung burden and

- 598 deposition distribution of inhaled atmospheric urban ultrafine particles as the first step in their
599 health risk assessment. *Atmos. Environ.* 104, 39–49. doi:10.1016/j.atmosenv.2014.12.060
- 600 Sánchez-Soberón, F., Mari, M., Kumar, V., Rovira, J., Nadal, M., Schuhmacher, M., 2015. An
601 approach to assess the Particulate Matter exposure for the population living around a cement
602 plant: modelling indoor air and particle deposition in the respiratory tract. *Environ. Res.* 143,
603 10–18. doi:10.1016/j.envres.2015.09.008
- 604 Schymanski, E.L., Jeon, J., Gulde, R., Fenner, K., Ruff, M., Singer, H.P., Hollender, J., 2014.
605 Identifying small molecules via high resolution mass spectrometry: Communicating
606 confidence. *Environ. Sci. Technol.* doi:10.1021/es5002105
- 607 Segawa, K., Nagata, S., 2015. An Apoptotic “Eat Me” Signal: Phosphatidylserine Exposure. *Trends*
608 *Cell Biol.* 25, 639–650. doi:10.1016/j.tcb.2015.08.003
- 609 Serfozo, N., Chatoutsidou, S.E., Lazaridis, M., 2014. The effect of particle resuspension during
610 walking activity to PM10 mass and number concentrations in an indoor microenvironment.
611 *Build. Environ.* 82, 180–189. doi:http://dx.doi.org/10.1016/j.buildenv.2014.08.017
- 612 Sharma, B., Kanwar, S.S., 2017. Phosphatidylserine: A cancer cell targeting biomarker. *Semin.*
613 *Cancer Biol.* doi:10.1016/j.semcancer.2017.08.012
- 614 Smith, C.A., O’Maille, G., Want, E.J., Qin, C., Trauger, S.A., Brandon, T.R., Custodio, D.E.,
615 Abagyan, R., Siuzdak, G., 2005. METLIN: a metabolite mass spectral database. *Ther. Drug*
616 *Monit.* 27, 747–51.
- 617 Stillwell, W., 2016. Membrane Polar Lipids, in: *An Introduction to Biological Membranes*. Elsevier,
618 pp. 63–87. doi:10.1016/B978-0-444-63772-7.00005-1
- 619 US EPA, 2016. Basic Information | Particulate Matter | Air & Radiation | US EPA [WWW
620 Document]. URL <https://www.epa.gov/pm-pollution/particulate-matter-pm-basics#PM>
621 (accessed 5.31.15).
- 622 Vaccari, M., Mascolo, M.G., Rotondo, F., Morandi, E., Quercioli, D., Perdichizzi, S., Zanzi, C.,
623 Serra, S., Poluzzi, V., Angelini, P., Grilli, S., Colacci, A., 2015. Identification of pathway-based

- 624 toxicity in the BALB/c 3T3 cell model. *Toxicol. Vitr.* 29, 1240–1253.
625 doi:10.1016/j.tiv.2014.10.002
- 626 van Drooge, B.L., Marqueño, A., Grimalt, J.O., Fernández, P., Porte, C., 2017. Comparative toxicity
627 and endocrine disruption potential of urban and rural atmospheric organic PM₁ in JEG-3
628 human placental cells. *Environ. Pollut.* 230, 378–386. doi:10.1016/j.envpol.2017.06.025
- 629 Vance, J.E., 2008. Thematic Review Series: Glycerolipids. Phosphatidylserine and
630 phosphatidylethanolamine in mammalian cells: two metabolically related aminophospholipids.
631 *J. Lipid Res.* 49, 1377–1387. doi:10.1194/jlr.R700020-JLR200
- 632 Vance, J.E., Tasseva, G., 2013. Formation and function of phosphatidylserine and
633 phosphatidylethanolamine in mammalian cells. *Biochim. Biophys. Acta - Mol. Cell Biol.*
634 *Lipids.* doi:10.1016/j.bbalip.2012.08.016
- 635 Viana, M., Rivas, I., Querol, X., Alastuey, A., Álvarez-Pedrerol, M., Bouso, L., Sioutas, C., Sunyer,
636 J., 2014. Partitioning of trace elements and metals between quasi-ultrafine, accumulation and
637 coarse aerosols in indoor and outdoor air in schools. *Atmos. Environ.* 106, 392–401.
638 doi:10.1016/j.atmosenv.2014.07.027
- 639 von Moos, N., Slaveykova, V.I., 2014. Oxidative stress induced by inorganic nanoparticles in
640 bacteria and aquatic microalgae – state of the art and knowledge gaps. *Nanotoxicology* 8, 605–
641 630. doi:10.3109/17435390.2013.809810
- 642 Wang, X., Jiang, S., Liu, Y., Du, X., Zhang, W., Zhang, J., Shen, H., 2017. Comprehensive
643 pulmonary metabolome responses to intratracheal instillation of airborne fine particulate
644 matter in rats. *Sci. Total Environ.* 592, 41–50. doi:10.1016/j.scitotenv.2017.03.064
- 645 Wheelock, C.E., Goss, V.M., Balgoma, D., Nicholas, B., Brandsma, J., Skipp, P.J., Snowden, S.,
646 Burg, D., D’Amico, A., Horvath, I., Chaiboonchoe, A., Ahmed, H., Ballereau, S., Rossios, C.,
647 Chung, K.F., Montuschi, P., Fowler, S.J., Adcock, I.M., Postle, A.D., Dahlén, S.-E., Rowe, A.,
648 Sterk, P.J., Auffray, C., Djukanovic, R., 2013. Application of ‘omics technologies to biomarker
649 discovery in inflammatory lung diseases. *Eur. Respir. J.* 42, 802–825.

- 650 doi:10.1183/09031936.00078812
- 651 WHO, 2014. WHO | Ambient (outdoor) air quality and health [WWW Document]. WHO. URL
652 <http://www.who.int/mediacentre/factsheets/fs313/en/> (accessed 6.21.16).
- 653 Wishart, D.S., Jewison, T., Guo, A.C., Wilson, M., Knox, C., Liu, Y., Djoumbou, Y., Mandal, R.,
654 Aziat, F., Dong, E., Bouatra, S., Sinelnikov, I., Arndt, D., Xia, J., Liu, P., Yallou, F., Bjorndahl,
655 T., Perez-Pineiro, R., Eisner, R., Allen, F., Neveu, V., Greiner, R., Scalbert, A., 2013. HMDB
656 3.0--The Human Metabolome Database in 2013. *Nucleic Acids Res.* 41, D801–D807.
657 doi:10.1093/nar/gks1065
- 658 Wu, W., Jin, Y., Carlsten, C., 2018. Inflammatory health effects of indoor and outdoor particulate
659 matter. *J. Allergy Clin. Immunol.* 141, 845. doi:10.1016/j.jaci.2018.01.014
- 660 Xia, J., Wishart, D.S., 2016. Using metaboanalyst 3.0 for comprehensive metabolomics data
661 analysis. *Curr. Protoc. Bioinforma.* 2016, 14.10.1-14.10.91. doi:10.1002/cpbi.11
- 662 Xia, T., Korge, P., Weiss, J.N., Li, N., Venkatesen, M.I., Sioutas, C., Nel, A., 2004. Quinones and
663 Aromatic Chemical Compounds in Particulate Matter Induce Mitochondrial Dysfunction:
664 Implications for Ultrafine Particle Toxicity. *Environ. Health Perspect.* 112, 1347–1358.
665 doi:10.1289/ehp.7167
- 666 Xiao, Y., Wang, L., Yu, M., Shui, T., Liu, L., Liu, J., 2018. Characteristics of indoor/outdoor
667 PM_{2.5} and related carbonaceous species in a typical severely cold city in China during heating
668 season. *Build. Environ.* 129, 54–64. doi:10.1016/j.buildenv.2017.12.007
- 669 Xu, W., Jiang, J., Yang, B., Mei, D., Dai, B., 2013. °. *Huanjing Kexue Xuebao/Acta Sci.*
670 *Circumstantiae* 33, 3407–3412.
- 671 Zhang, S.-Y., Shao, D., Liu, H., Feng, J., Feng, B., Song, X., Zhao, Q., Chu, M., Jiang, C., Huang,
672 W., Wang, X., 2017. Metabolomics analysis reveals that benzo[a]pyrene, a component of PM
673 2.5, promotes pulmonary injury by modifying lipid metabolism in a phospholipase A₂-
674 dependent manner in vivo and in vitro. *Redox Biol.* 13, 459–469.
675 doi:10.1016/j.redox.2017.07.001

- 676 Zimmermann, A., Bauer, M.A., Kroemer, G., Madeo, F., Carmona-Gutierrez, D., 2014. When less is
677 more : hormesis against stress and disease. *Microb. Cell* 1, 150–153. doi:doi:
- 678 Zinrajh, D., Hörl, G., Jürgens, G., Marc, J., Sok, M., Cerne, D., 2014. Increased
679 phosphatidylethanolamine N-methyltransferase gene expression in non-small-cell lung cancer
680 tissue predicts shorter patient survival. *Oncol. Lett.* 7, 2175–2179. doi:10.3892/ol.2014.2035
- 681 Zou, Y., Wu, Y., Wang, Y., Li, Y., Jin, C., 2017. Physicochemical properties, in vitro cytotoxic and
682 genotoxic effects of PM1.0 and PM2.5 from Shanghai, China. *Environ. Sci. Pollut. Res.* 24,
683 19508–19516. doi:10.1007/s11356-017-9626-9
- 684

Figure 1: Average levels of PM within the three microenvironments. Error bars denote standard deviations among samples (n=4). Asterisks denote statistically significant differences ($p < 0.05$).

Figure 2: Average daily share of time of the students attending to the school (n=20).

Figure 3: Dose-response graph of A549 cells after 72 h exposure to $PM_{2.5-0.25}$ (red) and $PM_{0.25}$ (blue). The curve was fitted using a two-phase decay. Error bars denote standard deviations (n=4). Characters indicate statistically significant differences between the two fractions at a given dose (a = $p < 0.05$; b = $p < 0.01$).

Figure 4: Hierarchical clustering heatmap analysis of significant differential metabolites after LC_5 exposure. Metabolite fold changes with respect to control cells range between deep blue (negative fold changes) to deep red (positive fold changes). Red dashed square embeds the control cluster, blue dashed square embeds the cluster comprising all $PM_{2.5-0.25}$ and one $PM_{0.25}$ replicate, and green dashed line embeds the remaining $PM_{0.25}$ replicates. Yellow dot-dashed square embeds those features mostly downregulated in exposed cells, while purple dot-dashed square embeds those features mostly upregulated in exposed cells.

Figure 5: Observed PS, PE, and PC changes after exposure to $PM_{2.5-0.25}$ (a) and $PM_{0.25}$ (b). Upregulated metabolites are shown in green background, while downregulated metabolites are shown in red. Key: Cho, choline; Etn, ethanolamine; PC, phosphatidylcholine; PE, phosphatidylethanolamine; PEMT, phosphatidyl-ethanolamine N-methyltransferase; PS, phosphatidylserine; Ser, serine.

Figure 6: Hierarchical clustering heatmap analysis of significant differential metabolites after real dose exposure. Metabolite fold changes with respect to control cells range between deep blue (negative fold changes) to deep red (positive fold

changes). Blue dashed square embeds most of the exposed replicates, while red dashed square embeds control cells plus remaining exposed replicates. Yellow dot-dashed square embeds those features mostly downregulated in exposed cells, while purple dot-dashed square embeds those features mostly upregulated in exposed cells.

ACCEPTED MANUSCRIPT

Table 1: Daily deposited doses calculated for every PM fraction and respiratory region ($\mu\text{g}/\text{day}$).

Activity	Environment	PM _{10-2.5}				PM _{2.5-0.25}				PM _{0.25}				Total
		Head	TB ¹	P ²	Total	Head	TB	P	Total	Head	TB	P	Total	
Sleeping	Home	11.24	5.44	0.3	16.98	1.6	0.34	2.4	4.34	4.98	1.3	5.7	11.98	33.31
Sitting	Classroom	18.88	8.51	0.17	27.56	3.21	0.71	4.45	8.37	5.86	1.46	6.35	13.67	49.6
Sitting	Home	7.55	3.41	0.07	11.03	1.07	0.24	1.48	2.79	3.3	0.82	3.57	7.69	21.5
Light intensity	Home	10.67	2.63	0	13.3	1.5	1	0.91	3.41	4.51	1.01	3.34	8.86	25.57
Light intensity	Outdoors	3.11	0.77	0	3.88	0.56	0.38	0.34	1.28	1.5	0.34	1.11	2.95	8.11
Heavy intensity	Outdoors	24.28	4.01	0	28.29	3.97	6.09	0.66	10.72	11.89	2.68	6.63	21.2	60.2
Total		75.72	24.77	0.54	101.03	11.91	8.75	10.25	30.91	32.05	7.6	26.7	66.35	198.29

¹ TB: Tracheobronchial; ² P: Pulmonary (Lung).

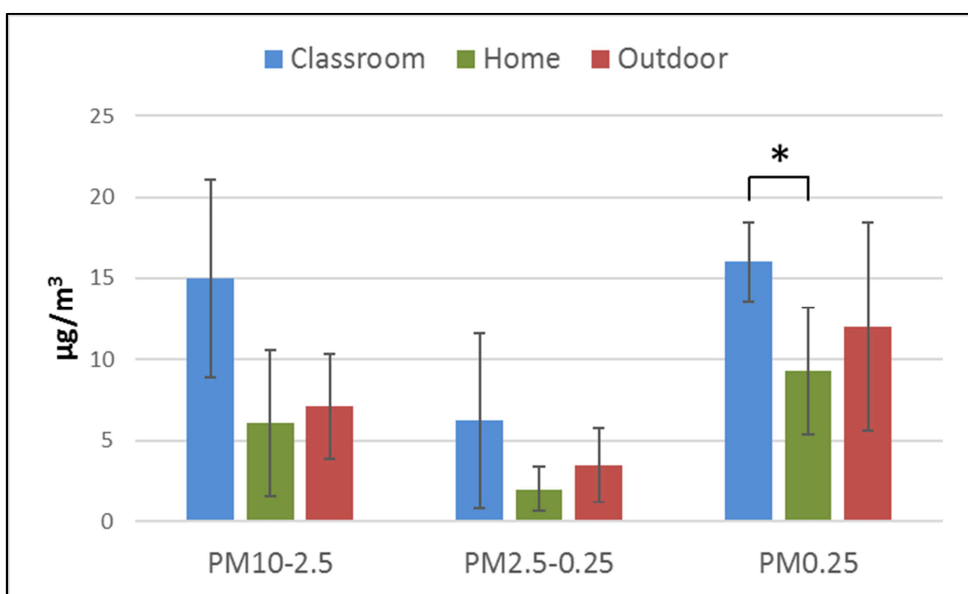


Figure 1

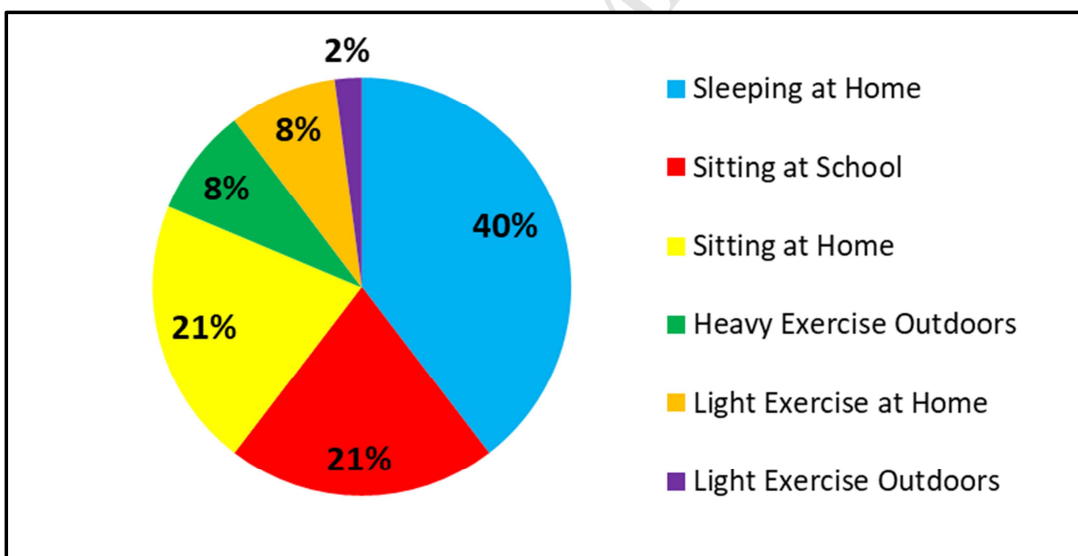


Figure 2

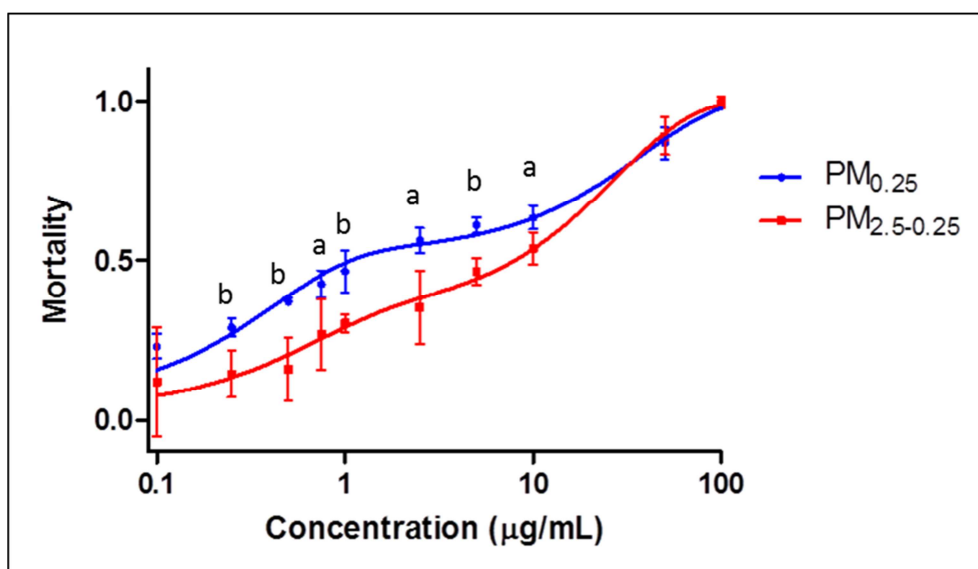


Figure 3

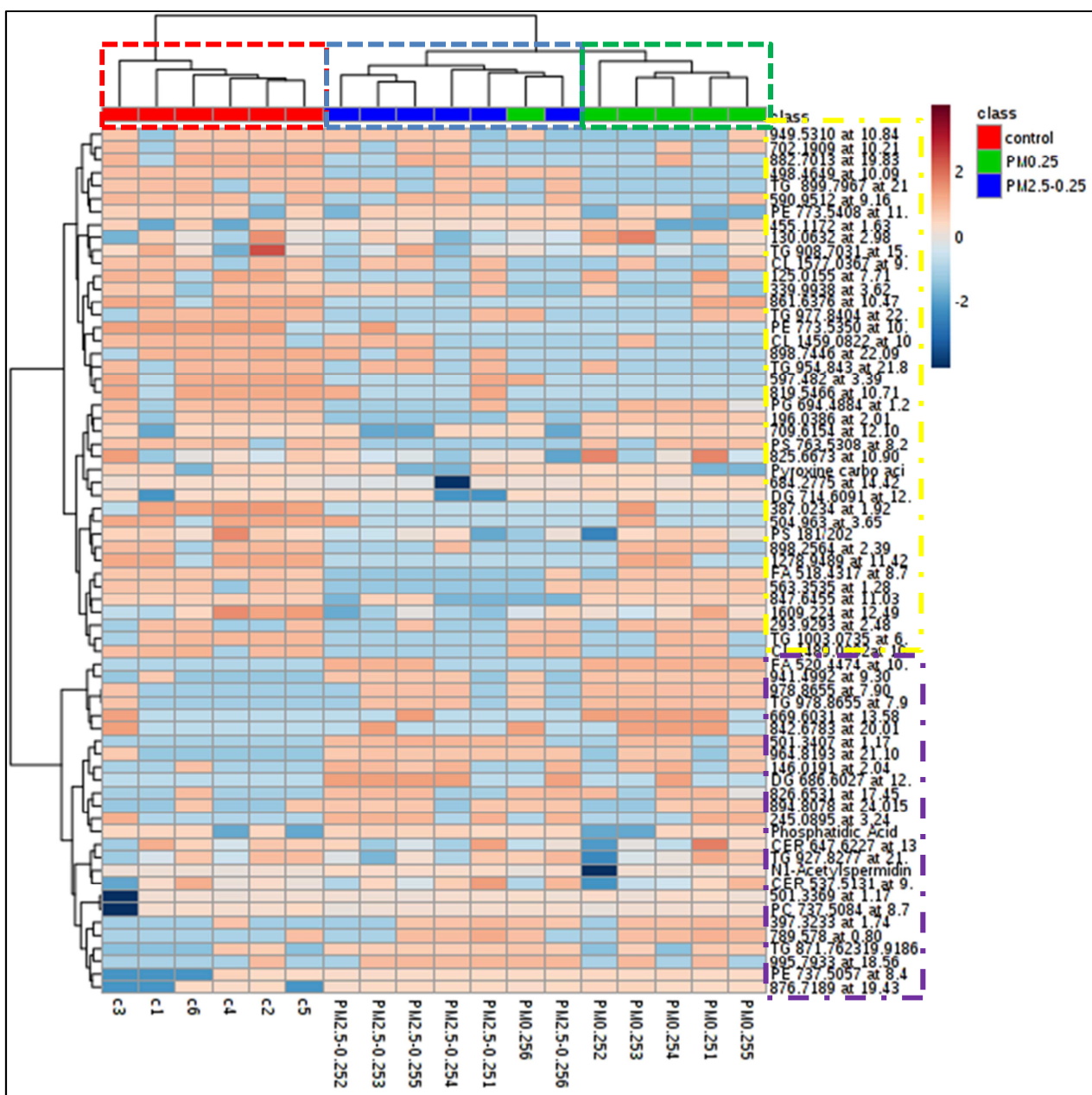


Figure 4

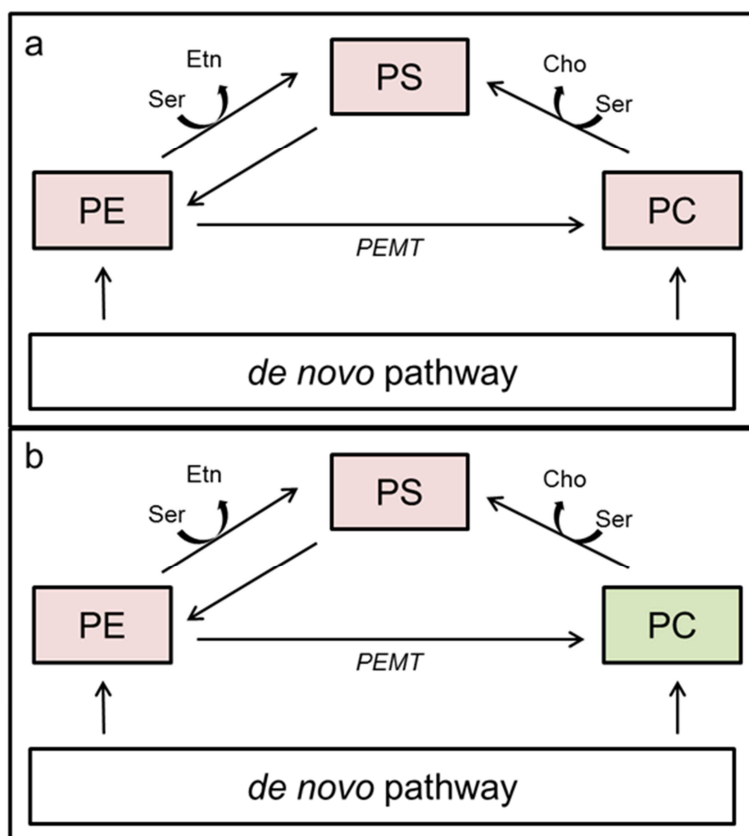


Figure 5

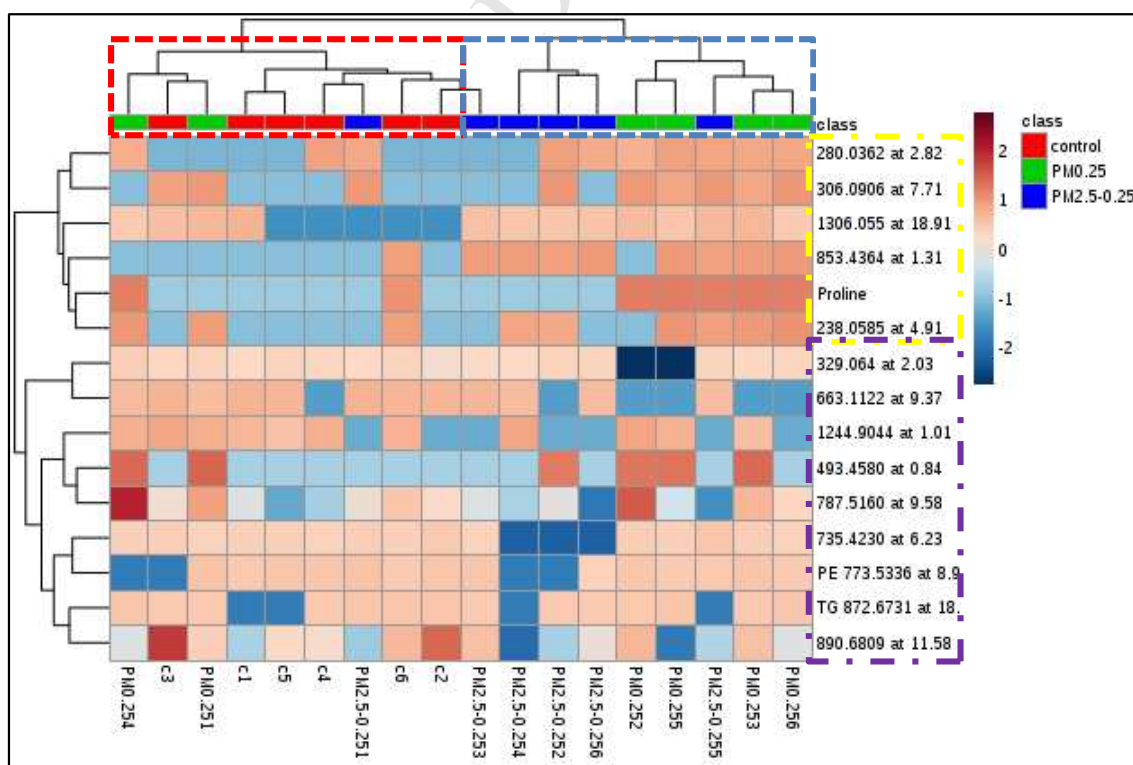


Figure 6

1 Highlights

- 2 • $PM_{10-2.5}$, $PM_{2.5-0.25}$, and $PM_{0.25}$ were sampled in indoor and outdoor
3 environments.
- 4 • Toxicity and metabolism of A549 cells exposed to $PM_{2.5-0.25}$ and $PM_{0.25}$ were
5 studied.
- 6 • $PM_{0.25}$ showed an overall higher toxicity than $PM_{2.5-0.25}$.
- 7 • $PM_{0.25}$ elicited a higher alteration in metabolism than $PM_{2.5-0.25}$.
- 8
- 9 • Most of the altered features were lipids present in cell and mitochondrial
10 membranes.